

## ***A Simplified Model for the Prediction of the Thermal Performance for Cross Flow Air Cooled Heat Exchangers with a New Air Side Thermal Correlation***

*Dr. Ali Hussain Tarrad*

*Mechanical Engineering Dept., College of Eng.  
Al-Mustansiriya University, Baghdad, Iraq*

*Lect. Ma'athe Abdul Wahed*

*Mechanical Engineering Dept., College of Eng.  
Al-Mustansiriya University, Baghdad, Iraq*

*Asst. Lect. Dhamia'a Saad Khudor*

*Mechanical Engineering Dept., College of Eng.  
Al-Mustansiriya University, Baghdad, Iraq*

### **Abstract**

*This investigation deals with the performance prediction of the cross flow air cooled heat exchangers. Experimental and theoretical studies were conducted to perform the optimization of the thermal design of the heat exchanger. The experimental work was carried out by two different types and sizes of finned tube air cooled heat exchangers. An experimental rig was built for this object which provides hot water at the range of (40 to 70) C° with water circulating rate of (200 to 1800) l/hr at absolute pressure of (2) bar. A centrifugal fan was installed as a major part of the experimental rig to provide atmospheric air with volumetric flow rate of (1250 and 2500) cfm.*

*The performance parameters measured in the experimental work were flow rates and temperature at the entering and leaving sides of the process and service fluids passing through the heat exchanger. Further, the water side operating pressure at the inlet and exit ports, and the wet bulb temperature of air on both sides of heat exchanger have been measured as well. The entering air dry bulb and wet bulb temperatures were in the range (16 to 24) C° and (13 to 20) C° respectively. The air leaving dry bulb and wet bulb temperatures were (23 to 40) C° and (15 to 26) C° respectively.*

*In the theoretical part of this work, a simplified correlation for the air side heat transfer coefficient for the cross flow heat exchangers was suggested in the present work. This formula was based on the dimensionless groups of the Buckingham-pi theorem. It was incorporated in the general formula for the overall heat transfer coefficient for the prediction of the heat exchanger performance. The discrepancy between the predicted and experimental values of the overall heat transfer coefficient and heat duty were within (2%) and (4%) respectively for both of the tested tube banks. The results of the present correlation of the air side heat transfer coefficient revealed a good agreement with that of the well known McQuiston method.*

## الخلاصة

يتعامل هذا البحث بالتنبؤ لأداء مبادلات حرارية مبردة بالهواء وذات الجريان المتقاطع. تم تنفيذ دراستين عملية ونظرية لإعداد التصميم الأمثل لهذه المبادلات. لتنفيذ الجانب العملي تم استخدام مبادلات مبردة بالهواء مختلفة من حيث النوع والحجم. تم بناء منظومة مختبرية لهذا الغرض تقوم بتجهيز الماء الساخن بمدى درجات حرارة يتراوح بين (٤٠) م<sup>°</sup> و (٧٠) م<sup>°</sup> وبمعدل جريان يقع ضمن المدى (٢٠٠) لتر/ساعة إلى (١٨٠٠) لتر/ساعة وبضغط مطلق مقداره (٢) بار. تم تثبيت دافعة هواء مركزية (Centrifugal Fan) كجزء رئيسي من المنظومة المختبرية لتزويد الهواء الجوي بمعدل جريان حجمي مقداره (١٢٥٠) قدم<sup>٣</sup>/دقيقة أو (٢٥٠٠) قدم<sup>٣</sup>/دقيقة.

متغيرات الأداء التي تم قياسها خلال التجارب العملية تمثل معدلات الجريان ودرجة حرارة الدخول والخروج لكل من المائع العملياتي والمائع الخدمي المار عبر المبادل الحراري. كذلك تم قياس الضغط التشغيلي للماء الساخن عند فتحات الدخول والخروج لجانب الأنابيب ودرجة حرارة البصلة الرطبة للهواء على جانبي المبادل. عند الدخول للمبادل تقع درجة حرارة البصلة الجافة والبصلة الرطبة للهواء ضمن المديات (١٦ إلى ٢٤) م<sup>°</sup> و (١٣ إلى ٢٠) م<sup>°</sup> على التعاقب. أما درجة حرارة البصلة الجافة والبصلة الرطبة للهواء عند جانب الخروج من المبادل فيقع ضمن المديات (٢٣ إلى ٤٠) م<sup>°</sup> و (١٥ إلى ٢٦) م<sup>°</sup> بالتعاقب.

بالجانب النظري لهذا البحث، تم اقتراح علاقة مبسطة لحساب معامل انتقال الحرارة لجانب الهواء للمبادلات ذات الجريان المتقاطع. لقد اعتمدت المعادلة المقترحة على نظرية (Buckingham-pi) للمجاميع اللابعديّة والتي تم تضمينها للمعادلة العامة لحساب معامل انتقال الحرارة الكلي عند التنبؤ بأداء المبادل الحراري. أعطت المعادلة المقترحة عند حساب معامل انتقال الحرارة الكلي والحمل الحراري فرقاً عن تلك المستحصلة تجريبياً بمقدار (٢%) و (٤%) على التعاقب لكلا المبادلين. النتائج التي تم الحصول عليها باستخدام العلاقة المقترحة عند حساب معامل انتقال الحرارة الكلي بينت تطابق جيد مع تلك المحسوبة بطريقة McQuiston الأكثر شيوعاً.

## 1. Introduction

Heat exchanger is a device, which is applied to transfer thermal energy between fluids at different temperatures, or is a device in which heat is transferred from a hot fluid to a cold fluid. In its simplest form, the two fluids mix and leave at an intermediate temperature determined from the conservation of energy, Kakac<sup>[1]</sup>. In most applications, the fluids do not mix but transfer heat through a separating wall which takes on a wide variety of geometries. Also heat exchanger is classified according to flow arrangement. Therefore, heat exchangers may have parallel, counter, or cross flow patterns for the process and service fluid flow directions, Sinnott<sup>[2]</sup>.

Fin-and-tube heat exchangers are widely used in several life fields such as heating, ventilating, refrigeration and air conditioning systems. A fluid is considered to have made one pass if it flows through a section of the heat exchanger through its full length. If the fluid is reversed and flows through an equal or different section, it is considered to have made a second pass of equal or different size. One of the major advantages of multi passing is to increase the exchanger overall effectiveness over individual pass effectiveness. The multipass arrangements are classified according to the type of construction, for example, extended surface, or plate's exchanger. Finned surfaces are often employed where the heat transfer coefficient readily attainable with one fluid stream is much higher than that readily attained with the other, for example, in gas to liquid heat exchangers. The use of finned surfaces is particularly advantageous when applied to tube banks in cross flow.

Many investigations have been conducted to predict the thermal and hydrodynamics performance of the cross flow heat exchangers. Brown<sup>[3]</sup> presented preliminary estimates for the thermal design for heat exchangers. He established a procedure in a tabulated form for the

design of heat exchangers with (3 to 6) rows bank of circular finned tubes. The design procedure requires the availability of the overall heat transfer coefficient for the heat exchanger prior to the commencing of the thermal design. Such values of the heat transfer coefficient may be obtained from literature as he suggested. Ganapathy <sup>[4]</sup> gave a procedure for the thermal and hydrodynamics design of circular finned tube banks. Still the design is based on an assumed overall heat transfer coefficient prior to the design strategy has commenced.

Saddler <sup>[5]</sup> investigated experimentally and theoretically the prediction of the thermal and hydraulic performance of an air conditioning unit for residential application. He presented a procedure for the prediction of all parameters tracing the performance of the individual components and showed the effect of different parameters on the thermal design of evaporator and condenser. Stewart et. al. <sup>[6]</sup> studied a space cooling system with a focus on the finned tube condenser design details. The finned tube heat exchanger, condenser was made of plate fins on circular tube cross section. An optimization algorithm was implemented to find the optimum design for 10 condenser design parameters using various constrains. The figure of the merit was system efficiency.

More recently Tarrad and Shehhab <sup>[7]</sup> have presented a procedure for the thermal and hydrodynamics design of the plate finned tube heat exchanger. A change of phase was considered in their study, they investigated the vaporization of refrigerant-22 in air cooled cross flow heat exchanger as a part of air conditioning unit. The study considered both regions on the refrigerant side, evaporation and superheating. In addition, the dehumidification of air as it passes across the heat exchanger was taken into account.

In the present study, the experimental data for cooling of water in a cross flow plate fin heat exchanger was obtained for two different types and sizes of radiators. A procedure is presented for the design of cross flow plate fin heat exchangers having single and multi tube passing. A correlation for the air side heat transfer coefficient is suggested and formulated by using a dimensional analysis based on the Buckingham-pi theorem for the dimensionless groups. The results of this investigation can be used for the prediction of heat exchanger size employed in the heating season for air conditioning application in addition to the power plants and oil industry fields.

## **2. Experimental Work and Results**

The constructed test rig is shown schematically in **Fig.(1)**. It consists of a test section which is a model of a plate finned tube heat exchanger, water reheater, water pumping system, control panel and measuring instrumentation. The rig is made of steel structure on which the testing component is fixed.

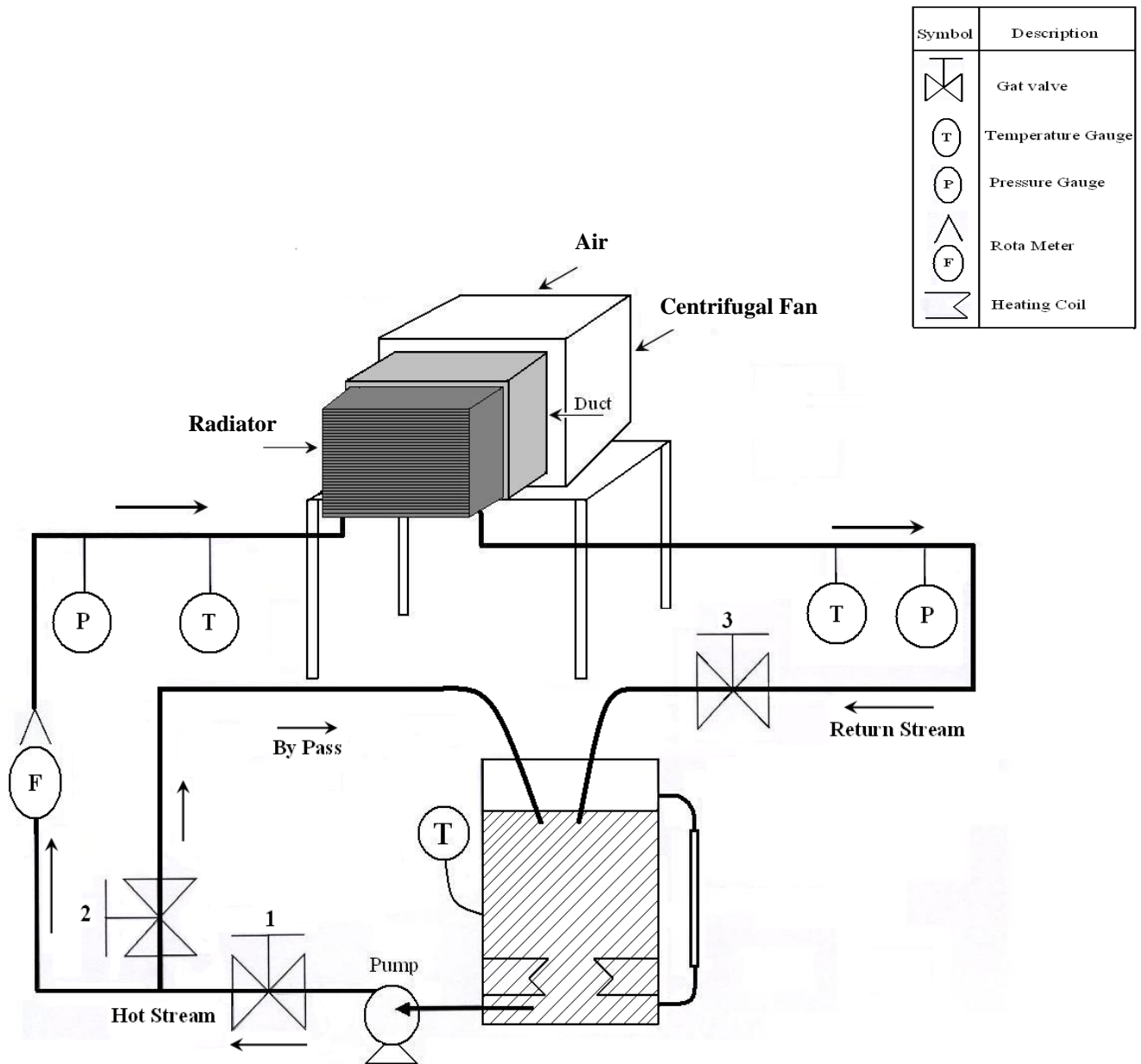


Figure (1) A schematic diagram of the experimental rig.

## 2-1 Heat Exchanger

There are two type of test section. The first type is made of single pass finned tube heat exchanger, having dimensions of (40cm) overall length, which contains (34) copper tube of (13mm) slot length and (3mm) slot width, and fins number are (52), with fin pitch (4 fin/in), and fins thickness (0.5mm). The tubes are elliptical cross section distributed as a triangular tube pattern. The clearance between two adjacent tubes is (3 mm), and the tubes pitch in the transverse and longitudinal directions to the flow are (12 mm) and (16 mm) respectively. The total frontal area of the heat exchanger is (40×40.5 cm<sup>2</sup>), with a width of (6.5 cm), **Fig.(2.a)**.

The second type is made of multi tube passes plate finned tube heat exchanger, having dimensions of (400 mm) overall length, which contains (16) copper tube per pass. The inner tube diameter is (7mm) and (9mm) outer diameter. Total fins number are (160), with fin pitch (8 fin/in), and fin thickness of (0.2mm). The tubes are distributed in a triangular tube pattern. The tubes pitch in the transverse and longitudinal directions to the air flow are (25mm) and (30 mm) respectively. The heat exchanger total frontal area is (40×29 cm<sup>2</sup>) with a width of (4.5cm), **Fig.(2.b)**.

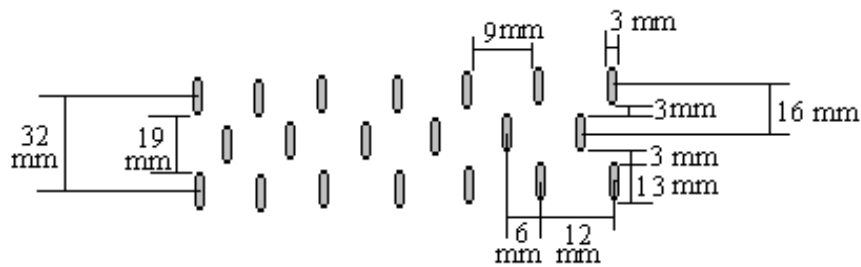
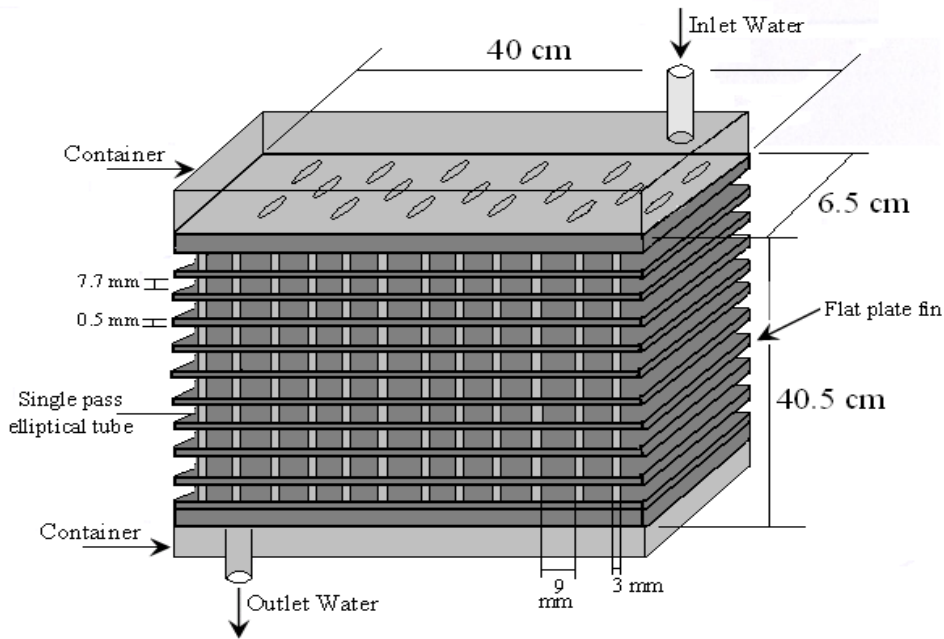
The finned tube heat exchanger is designed for cross flow configuration, in which the hot water flows in the tubes in perpendicular direction to the cold air stream flows on air side, pressure gauge are connected to the inlet and outlet tube sides. The connections are insulated with a glass wool insulation mat of (10mm) thickness, in order to reduce heat loss to the minimum level.

## **2-2 Water Feeding Systems**

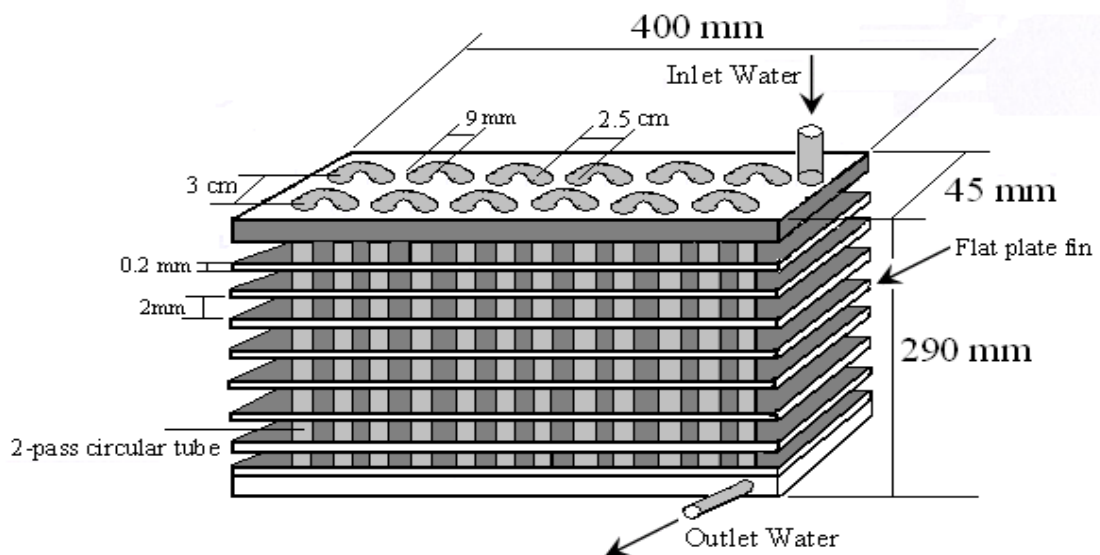
The hot water is supplied by a constant head tank of (250 liters) capacity heating tank through the test section and it returns back to the heating tank or reheater. The water in the reheater is heated by four electrical heaters, which have a total heating electrical power of (12 kW). The four heaters are fixed at the base of the reheater at (150mm) from the bottom. The hot water intake connection is made at (70mm) from the bottom of the reheater. This arrangement of heaters with the use of rated thermostat of an average range of (30-80C°) will help in providing a good control over the water temperature during test. Hot water flow is controlled by globe valves and the flow is measured by using a vertical variable area rotameter. The hot water side circulation pipes are lagged by (10mm) glass wool insulation mat in order to reduce the hot loss for the whole hot circulation system.

## **2-3 Air Circulation System**

The air was supplied to the test heat exchanger through a centrifugal fan and ducting system. A forced draught arrangement was selected for the test object. An air cooler with a maximum capacity of (2500) cfm was installed close enough to the test section to avoid leakage of air to the surrounding. The air supply unit has two different volumetric flow rate levels controlled manually by using variable speed motor to provide (50%) of the maximum value. It was installed on the top of a steel structure kept in horizontal position as shown in **Fig.(1)**.



a) Large radiator: single-pass elliptical tube



b) Small radiator: Multi-pass circular tube

Figure (2) The cross flow heat exchanger specifications used in the present work

## **2-4 Measuring Instrumentation**

### **2-4-1 Water Measurements**

The parameters to be measured during tests for the water side are:

1. The inlet and outlet temperatures, (C°).
2. The inlet and outlet pressures, (C°).
3. The water volumetric flow rate, (l/hr).

A vertical variable area rotameter is used to measure the flow rate of the hot water with the range of (200-1900) l/hr.

### **2-4-2 Air Measurements**

The air side parameters to be measured during the tests are:

1. The entering and leaving dry-bulb temperatures, (C°).
2. The entering and leaving wet-bulb temperatures, (C°).
3. The volumetric flow rate, (cfm).

All of the temperature measurements were obtained by calibrated temperature gauges against a standard mercury thermometer with a maximum deviation percentage of (0.1%). Air flow rate was measured by the use of air flow meter in addition to the known value of the volumetric flow from the setting of the air cooler.

The electrical board which supplies the electrical power to the whole system components of the test rig consists of an electrical contactor of (4×16 Amp), which is connected to the four heaters and the thermostat.

## **2-5 Test Procedure**

After completing checking system, the test process begins by switching on the circuit breaker that supplies power to the whole system. Then the electrical power will transfer to heaters which will raise the temperature of water in the reheater as required to the desired temperature fixed by setting the thermostat. This process takes (10-20) minutes depending upon the required temperature from the thermostat and the temperature of water before starting. After that, the hot water pump will start and open the gate valve that controls the flow rate of hot water which flows on the tube side of the test heat exchanger. The thermostat controls the electrical power supplied to the four heaters to cover the temperature dropping in the system until reaching the desired temperature. This process normally takes (10-15) minutes depending upon the required temperature and the flow rate. On the air side, switch on the air centrifugal fan, at the same time of the hot water pumping and the flow is set according to the required flow rate. These operations normally take about (20-35) minutes as an overall time to reach the steady state condition.

Then air volumetric flow rate is fixed at (1250) cfm, at the required entering temperature of the hot water set by the thermostat. On the water side (tube side), flow rate of water is regulated and changed from (800) l/hr to (1800) l/hr for the large radiator and (200) l/hr to

(400) l/hr for the small one. Water temperatures are continuously measured during flow rate variation and also the pressures are measured at the inlet and the outlet of the exchanger at known flow rate for the tube side. Any test reading taken for the above mentioned procedure is repeated and recorded four times at a time interval of (5) minute step. The same data was obtained at air flow rate of (2500) cfm.

Tests are repeated after changing setting of the thermostat by (5)C° step from temperature setting level of (40 up to 65 C°). During each step of test, the flow rate of water is regulated and temperature and pressure are taken. Analysis and comparison of readings results are carried out at different conditions. **Table (1)** shows the characteristics of the experimental work carried out during this investigation.

**Table (1) The variables range of the experimental work**

Heat Exchanger Size and Number	Entering Water Temp. (C°)	Entering Air Temp. (C°)	Water Flow Rate (l/hr)	Air Flow Rate (cfm)
Small No. (1)	40 ----- 65	22 ----- 23	200 ----- 400	1250--- 2500
Large No. (2)	40 ----- 65	16 ----- 24	800 ----- 1800	1250--- 2500

## 2-6 Experimental Results

**Table (2)** shows a sample of the data obtained for the cooling process for the large finned tube heat exchanger. These data was collected for water flow rate of (1800) l/hr at air volumetric flow rates of (1250) cfm and (2500) cfm. The corresponding data for the small finned tube bank are shown in **Table (3)** for water flow rate of (400) l/hr at the above air flow rates at temperature range between (40) and (65) C°.

The most important factors outline the performance of the heat exchanger are the tube bank heat duty, Q, the overall heat transfer coefficient, U<sub>o</sub>, and the effectiveness, ε. These parameters were calculated from the data collected in this investigation.

**Table (2.a) The experimental data of the large tube bank at air flow rate of (1250) cfm and water flow rate of (1800) l/hr**

T <sub>wi</sub> (C°)	P <sub>wi</sub> (bar)	T <sub>wo</sub> (C°)	P <sub>wo</sub> (bar)	T <sub>adi</sub> (C°)	T <sub>awi</sub> (C°)	T <sub>ado</sub> (C°)	T <sub>awo</sub> (C°)
40	0.16	37.7	0.08	18	14	26	17
45	0.16	42	0.08	18	14	28	17
50	0.16	46.5	0.08	18	14	30	18
55	0.16	51	0.08	18	14	32	19
60	0.16	55.7	0.08	18	14	33	19
65	0.16	60	0.08	18	14	35	20

**Table (2.b) The experimental data of the large tube bank at air flow rate of (2500) cfm and water flow rate of (1800) l/hr**

$T_{wi}$ (C°)	$P_{wi}$ (bar)	$T_{wo}$ (C°)	$P_{wo}$ (bar)	$T_{adi}$ (C°)	$T_{awi}$ (C°)	$T_{ado}$ (C°)	$T_{awo}$ (C°)
40	0.2	36	0.11	22	13	29	16
45	0.2	40.4	0.11	22	13	30	16
50	0.2	44.3	0.11	22	13	32	17
55	0.2	48.7	0.11	22	13	33	17

**Table (3.a) The experimental data of the small tube bank at air flow rate of (1250) cfm and water flow rate of (400) l/hr**

$T_{wi}$ (C°)	$P_{wi}$ (bar)	$T_{wo}$ (C°)	$P_{wo}$ (bar)	$T_{adi}$ (C°)	$T_{awi}$ (C°)	$T_{ado}$ (C°)	$T_{awo}$ (C°)
40	0.16	30	0.12	22	18	33	22
45	0.16	32	0.12	22	18	35	23
50	0.16	36	0.12	22	18	36	24
55	0.16	38	0.12	22	18	38	24
60	0.16	42	0.12	22	18	39	25
65	0.16	46	0.12	22	18	40	26

**Table (3.b) The experimental data of the small tube bank at air flow rate of (2500) cfm and water flow rate of (400) l/hr**

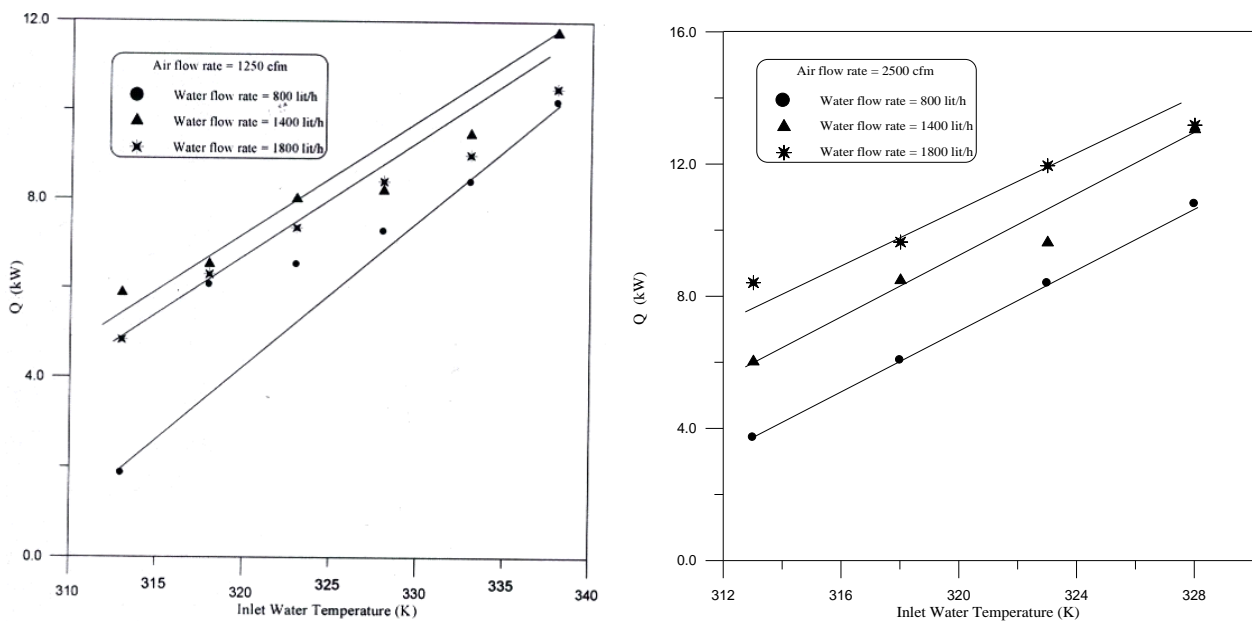
$T_{wi}$ (C°)	$P_{wi}$ (bar)	$T_{wo}$ (C°)	$P_{wo}$ (bar)	$T_{adi}$ (C°)	$T_{awi}$ (C°)	$T_{ado}$ (C°)	$T_{awo}$ (C°)
40	0.16	33.5	0.1	23	20	27	22
45	0.16	36	0.1	23	20	28	23
50	0.16	38.5	0.1	23	20	29	24
55	0.16	42	0.1	23	20	29.5	24
60	0.16	46	0.1	23	20	30	25
65	0.16	48	0.1	23	20	31	26

**2-6-1 Heat Duty**

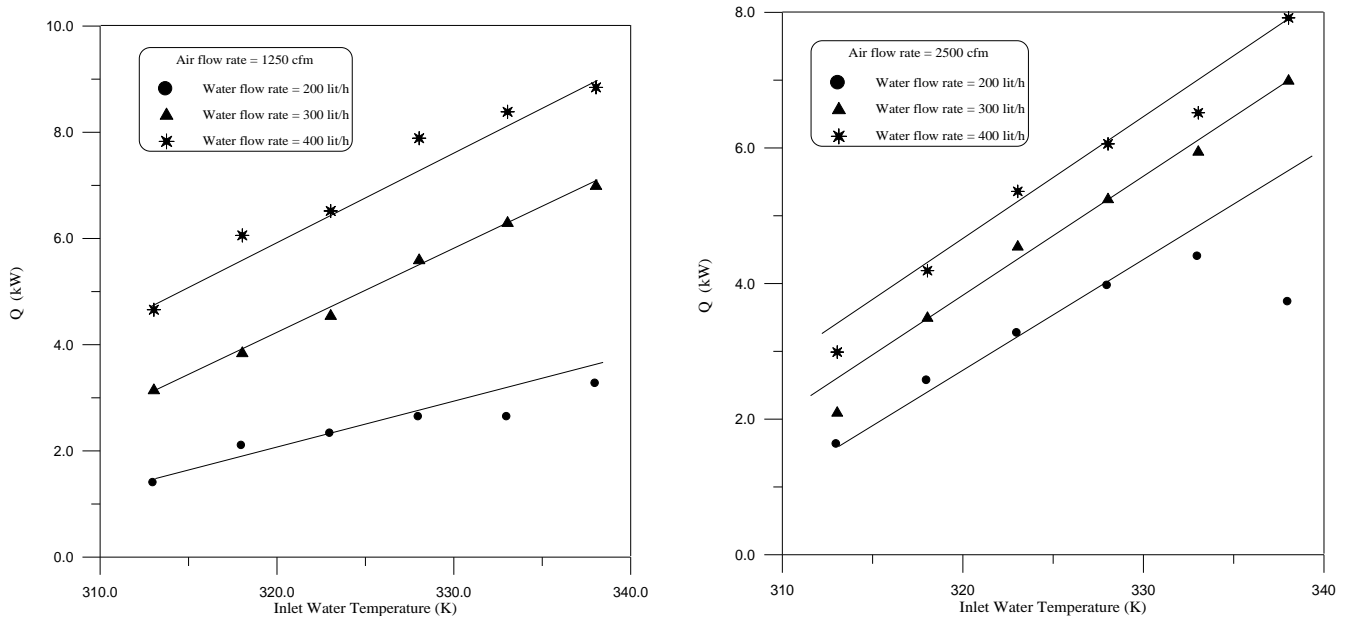
Figure (3) shows the variation of the cooling load of the heat exchanger with process fluid water flow rate; at different air volumetric flow passing through the tube bank of the large radiator no. (2). It is obvious that the general trend of the results shows that increasing the water flow rate passing through the heat exchanger produces an increase for the heat duty at specified entering water temperature. This is mainly due to high improvement in the tube side heat transfer coefficient,  $h_i$ , and its reflected effect on the heat exchanger performance. The measured cooling load of the heat exchanger is ranged from (4) to (10) kW when the

circulation water flow rate was ranged from (800) to (1800) l/hr at air flow rate of (1250) cfm. The corresponding values of heat duty and water flow rates for the small radiator no. (1) were ranged from (1.8) to (11) kW and (200) to (400) l/hr respectively. **Table (4)** shows the characteristics of the experimental data and its operating conditions of the present work.

Further, increasing the air side flow rate causes an improvement in the heat duty of the tube bank due to the improvement of the air side heat transfer coefficient,  $h_o$ . This of course is a result of improving the flow criteria through the finned surface and increasing the turbulence between the plate fins which is reflected in heat exchanger performance improvement.



**a) Large tube bank-single tube pass**



b) Small tube bank-multi tube passes

Figure (3) The variation of the heat exchanger load with water inlet temperature

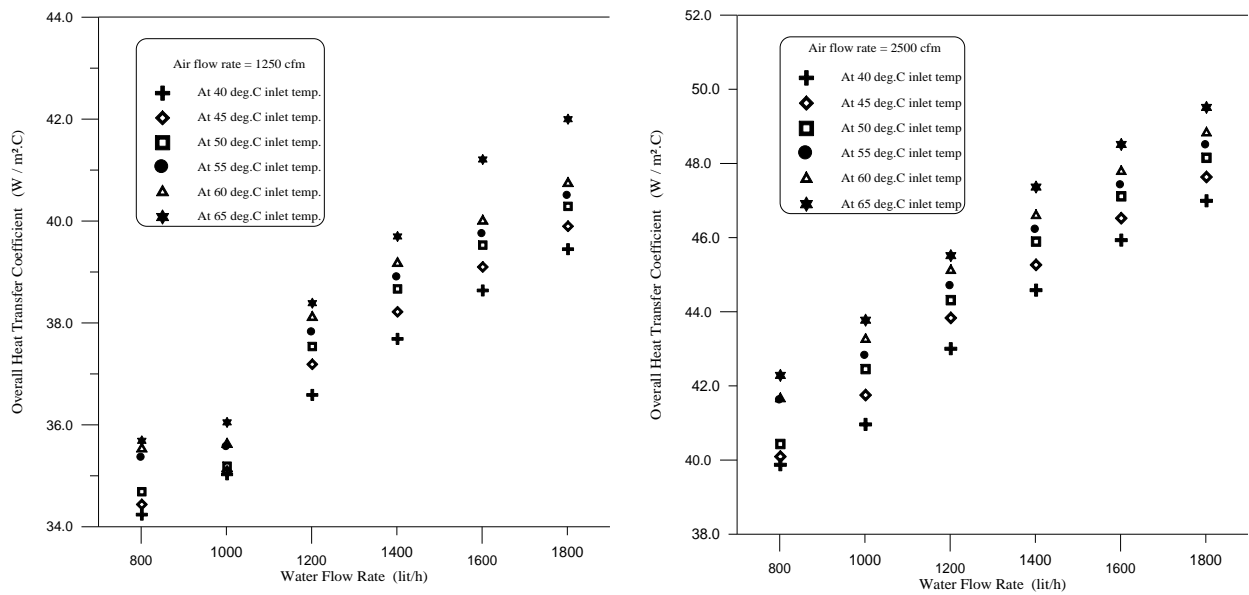
Table (4) The variables range of the experimental data of the present work

Heat Exchanger Size and Number	Inlet Water Temp. (C°)	Inlet Air Temp. (C°)	Exit Air Temp. (C°)	Air Flow (cfm)	Q <sub>cooling</sub> (kW)
Small No. (1)	40 ---- 65	22 ---- 23	25 ---- 40	1250	1.5 --- 9
	40 ---- 65	22 ---- 23	24 ---- 31	2500	1.5 --- 8
Large No. (2)	40 ---- 65	16 ---- 18	23 ---- 35	1250	2----11
	40 ---- 55	22 ---- 24	27 ---- 34	2500	4----13

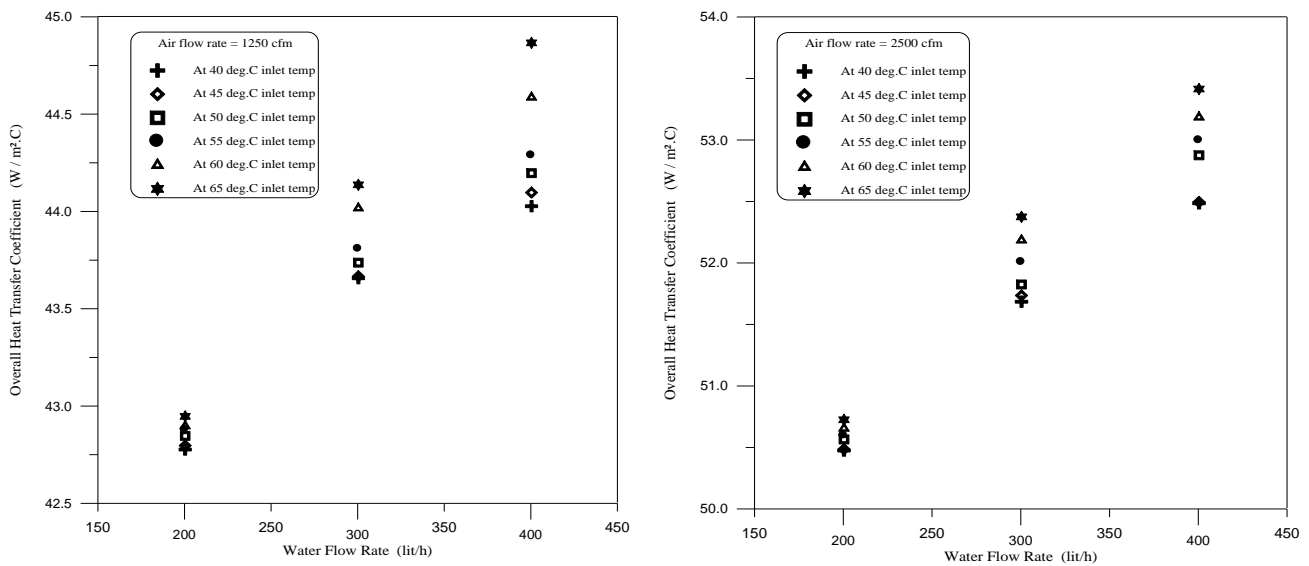
### 2-6-2 Overall Heat Transfer Coefficient

The variation of the overall heat transfer coefficient,  $U_o$ , of the finned tube banks with water flow rate entering the heat exchanger considered in this work is shown in **Fig.(4)**. It is clear that the trend of these curves shows an increase in the overall heat transfer coefficient with the increase of the flow rate of the circulated water, air volumetric flow rate, exposed area of heat exchanged and the temperature of both fluids at the entering section. In the large tube bank, radiator no. (2), the values of ( $U_o$ ) are ranged from (34) to (41)  $W/m^2 K$  for the whole range of the water inlet temperature and flow rates tested for the heat exchanger at air flow rate of (1250) cfm. The corresponding values for air flow rate of (2500) cfm were ranged from (40) to (50)  $W/m^2 K$  for the whole range of water side conditions. This is clearly due to the increasing values of the heat transfer coefficient on the air side. This was a result of the turbulence introduced by increasing the air velocity between fins.

The same argument may be inferred from the small tube bank, radiator no. (1), as shown in **Fig.(4)** but with different magnitudes. The range of ( $U_o$ ) was quite narrow for this radiator due to the small range of water tested, it was between (200) and (400) l/hr due to the heat exchanger size limitation. However, **Fig.(4)** shows that the range of ( $U_o$ ) for air flow of (1250) cfm was between (42) and (44)  $W/m^2 K$  and in the range of (50) to (53)  $W/m^2 K$  for the air flow of (2500) cfm. For this radiator, it can be concluded that the overall heat transfer coefficient for a specified air flow rate is almost constant in spite of the water flow rate is increased for the whole range of entering temperature.



**a) Large tube bank-single tube pass**



**b) Small tube bank-multi tube passes**

**Figure (4) The variation of the heat exchanger overall heat transfer coefficient with water flow rate at various entering temperature**

**2-6-3 Heat Exchanger Effectiveness**

The effectiveness is the ratio of the actual amount of heat transferred to the maximum possible amount of heat transferred during the operation of the heat exchanger.

$$\epsilon = \frac{Q_{\text{actual}}}{Q_{\text{maximum}}} \dots\dots\dots (1.a)$$

In which

$$Q_{\text{act}} = Q = \dot{m}_h c_{p_h} \Delta T_h = \dot{m}_c c_{p_c} \Delta T_c \dots\dots\dots (1.b)$$

and

$$Q_{\text{max}} = c_{\text{min}} \times (T_{hi} - T_{ci}) \dots\dots\dots (1.c)$$

The heat capacity, *c*, the extensive equivalent of the specific heat, determines the amount of heat a substance absorbed or rejected per unit temperature change.

$$c_{\text{min}} = \dot{m} \times cp \dots\dots\dots (1.d)$$

For a cross-flow heat exchanger with both fluids unmixed, the effectiveness can be related to the number of transfer unit (NTU) with the following equation.

$$\epsilon = 1 - \exp\left[\left(\frac{1}{c_r}\right)(NTU)^{0.22} \left[\exp(-c_r (NTU)^{0.78}) - 1\right]\right] \dots\dots\dots (1.e)$$

Where the heat capacity ratio (*c<sub>r</sub>*) is presented in equation:

$$c_r = \frac{c_{\text{min}}}{c_{\text{max}}} \dots\dots\dots (1.f)$$

The (NTU) is a function of the overall heat transfer coefficient in the form:

$$NTU = \frac{U_o \times A_o}{c_{\text{min}}} \dots\dots\dots (1.g)$$

The calculated effectiveness,  $\epsilon$ , by equations (1.a) to (1.d) and its variation with the (NTU), eq.(1.g), for different values of,  $c_r$ , of the finned tube cross flow heat exchanger are presented in **Fig.(5)** for both radiator geometries. The data shows that increasing the (NTU) number for a specified ( $c_r$ ) causes an increase in the ( $\epsilon$ ) values of the heat exchanger. For any value of (NTU), a reduction in the ( $c_r$ ) value reveals an increase in the heat exchanger

effectiveness ( $\epsilon$ ). When ( $c_r$ ) was reduced from (1.0) to (0.4) at (NTU) value of (3), produced an increase in the heat exchanger effectiveness ( $\epsilon$ ) from (33 to 41%) for the large tube bank, **Fig.(5.a)**. The corresponding values of the small tube bank were (37%) and (43%) respectively, **Fig.(5.b)**. The percentage of increase in the ( $\epsilon$ ) for the large and small tube banks considered in the present work were (20%) and (14%) respectively, calculated by:

$$\Delta\epsilon\% = \frac{\epsilon_{0.4} - \epsilon_{1.0}}{\epsilon_{0.4}} \times 100$$

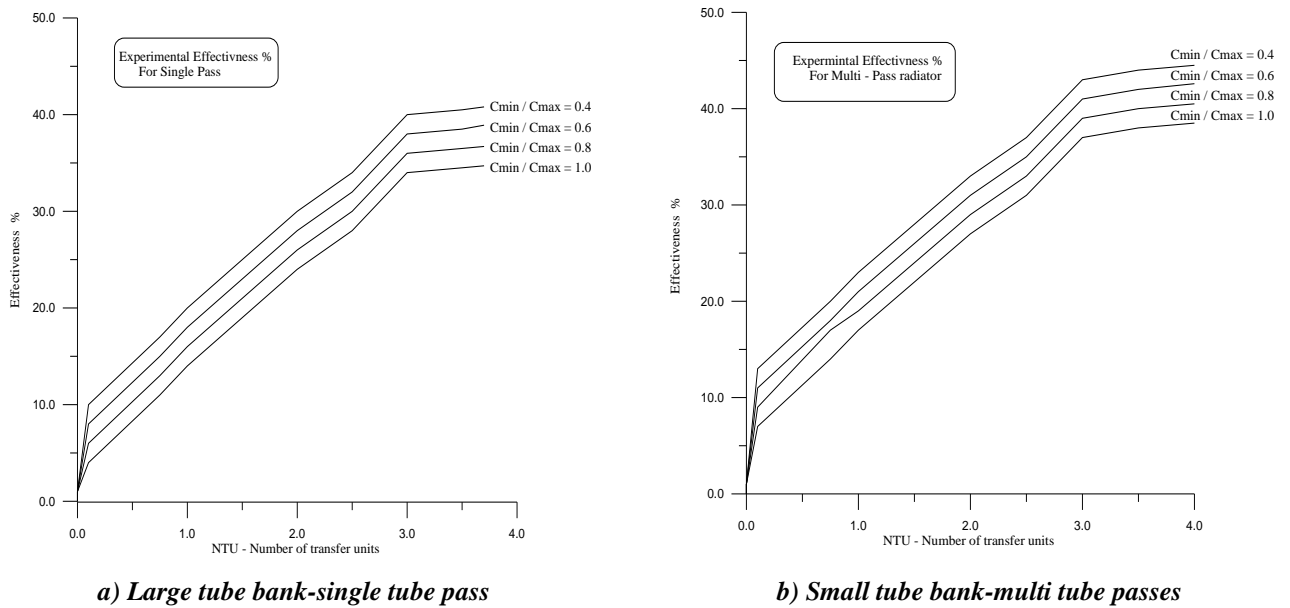


**Figure (5) The experimental heat exchanger effectiveness at different values of ( $c_r$ )**

### 3. Theoretical Analysis

This section deals with an overview and current development in the calculation for a single and multipass finned tube heat exchanger. The heating and cooling loads of a heat exchanger under operation conditions can be calculated from the knowledge of the flow rate and the temperature difference for each of heating and cooling side respectively from the equations:

$$Q_h = \dot{m}_h c_{p_h} \Delta T_h \dots\dots\dots (2.a)$$

$$Q_c = \dot{m}_c c_{p_c} \Delta T_c \dots\dots\dots (2.b)$$

The first step in the thermal and hydraulic design of the heat exchanger is to calculate the overall heat transfer coefficient ( $U_o$ ) which will be based on the air- side area. The overall

heat transfer coefficient, ( $U_o$ ) takes into consideration total thermal resistance to heat transfer between two fluids and neglecting the conduction and air side fouling resistances is presented by:

$$\frac{1}{U_o} = \frac{1}{h_o \eta_{so}} + \frac{1}{h_i (A_i/A_o)} + \frac{1}{h_f (A_i/A_o)} \dots\dots\dots (3)$$

The last term of the above expression represents the effect of the fouling resistance of the liquid stream passing through the heat exchanger coil. Its magnitude may be obtained experimentally or from tabulated data in the literature for the specified process fluid. In this work a value of (3000) W/m<sup>2</sup> K for the fouling effect,  $h_f$ , on the water side was used, Sinnott<sup>[2]</sup>.

**3-1 Water Side**

The recommended correlation presented by Sieder and Tate<sup>[8]</sup> for predicting the heat transfer coefficient in laminar flow in tubes may be used:

$$\frac{h_i D_i}{k_w} = 1.86 \left[ Re_w Pr \frac{D_i}{L} \right]^{1/3} \left( \frac{\mu_w}{\mu_s} \right)^{0.14} \dots\dots\dots (4)$$

Where the Reynolds number based on the tube inside diameter is:

$$Re_w = \frac{\rho_w u_w D_i}{\mu_w}$$

And the Prandtl number is expressed as:

$$Pr = \frac{\mu_w c_{p_w}}{k_w}$$

The above equation is applied for Reynolds number below 2100 where the flow is considered to be laminar. For Reynolds number higher than this value, the flow regime will be in the turbulent region and the Dittus-Boelter<sup>[9]</sup> is used in the form:

$$\frac{h_i D_i}{k_w} = 0.0243 Re_w^{0.8} Pr^n \dots\dots\dots (5)$$

In which the Prandtl number index (n) is equal to (0.4) for heating and (0.3) for cooling process.

These correlations are intended to be for the circular tube section. For noncircular tube sections, it is suggested in the present work to use an equivalent diameter deduced from the assumption of the same fluid velocity and flow rate for both tube section shapes. That is the

cross sectional area of the circular tube required to produce the same velocity and flow rate of fluid passing through the noncircular tube side.

**3-2 Air Side**

The work of McQuiston [10], was used with some modification to evaluate the air side convective heat transfer coefficient for a plate fin heat exchanger with multiple rows of staggered tubes. **Figure (6)** shows a schematic diagram for the plate fin heat exchanger considered in this investigation.

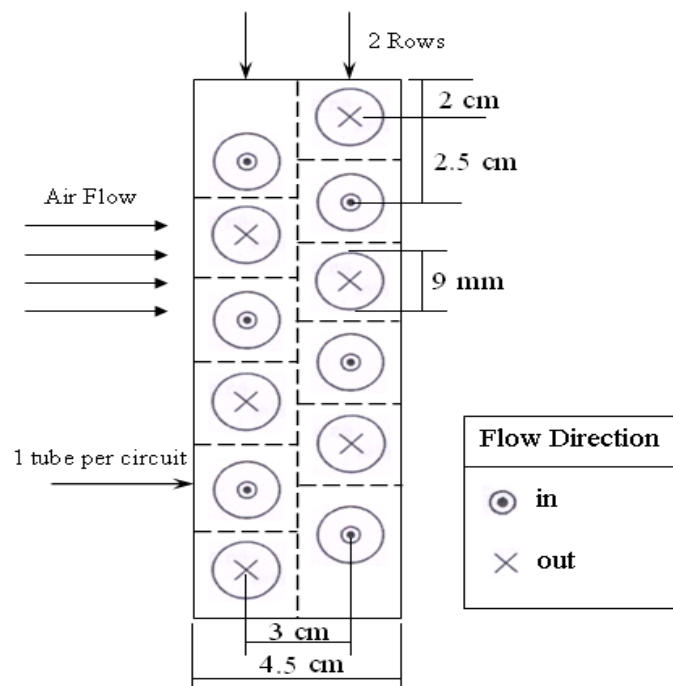


**Figure (6) Schematic diagram for multi tube Pass plate finned tube bank**

The Reynolds number based on the row spacing in the direction of air stream  $(Re_L)_a$  is defined by:

$$(Re_L)_a = \frac{G_{max} \times X_L}{\mu_a} \dots\dots\dots (6.a)$$

where, the mass velocity through minimum flow area ( $G_{max}$ ) is presented in:

$$G_{max} = \frac{\dot{m}_a}{A_{min}} \dots\dots\dots (6.b)$$

For cases in this study, the minimum flow area is:

$$A_{min} = W \times (1 - fp \times t) \times (H - (\tau_p \times N_{circ} \times D_o)) \dots\dots\dots (6.c)$$

Substituting the appropriate values for the Stanton number gives this relationship for the convective heat transfer coefficient

$$h_o = \frac{j \times c_{p_a} \times G_{max}}{(Pr)^{2/3}} \dots\dots\dots (7.a)$$

Here, in this work it is suggested to employ the air specific heat with modification to include the humidity handled by the air stream as it passes through the heat exchanger. Therefore, the humid heat of the air,  $c_{p_{hum}}$ , will be used instead of the dry air specific heat in eq.(6.a) with a value of (1.02) kJ/kg.K.

The heat transfer coefficient of air is based on the Colburn j-factor which is defined as:

$$j = St \times (Pr)^{2/3} \dots\dots\dots (7.b)$$

The heat transfer coefficient for heat exchangers with four or less rows can be found using the following correlation:

$$\frac{j_n}{j_4} = \frac{1 - (1280)(n)(Re_L)_a^{-1.2}}{1 - (1280)(4)(Re_L)_a^{-1.2}} \dots\dots\dots (7.c)$$

McQuiston found that the j-factor for a four row finned-tube heat exchanger fits a linear model based on the parameter (JP).

$$j_4 = 0.2675 \times JP + 1.325 \times 10^{-6} \dots\dots\dots (7.d)$$

and,

$$JP = Re_D^{-0.4} \times \left( \frac{A_o}{A_t} \right)^{-0.15} \dots\dots\dots (7.e)$$

Here ( $A_t$ ) represents the area of the bare tubes without fins and ( $A_o$ ) is the total air side heat transfer area, fins and tubes. The Reynolds number is based on the outside tube diameter and the maximum mass velocity, at minimum flow area of the tube bank.

To find out the overall surface efficiency for finned tube heat exchanger, it is necessary to determine the efficiency of the fins alone. The total air side surface efficiency is given by:

$$\eta_{so} = 1 - \frac{A_f}{A_o} \times (1 - \eta_f) \dots\dots\dots (8.a)$$

In this formula, ( $A_f$ ) represents the total fin surface area. The fin efficiency ( $\eta_f$ ) for a circular fin is a function of ( $m$ ,  $r_e$  and  $\phi'$ ).

$$\eta_f = \frac{\tanh (m \times r_e \times \phi')}{(m \times r_e \times \phi')} \dots\dots\dots (8.b)$$

Schmidt <sup>[11]</sup> analyzed hexangular and rectangular plate fin tube array and determined that they could be treated like circular fins by replacing the outer dimension of the fin with an equivalent radius, **Fig.(7)**. His method is based on the selection of a circular fin with a radius ( $r_e$ ) that has the same fin efficiency as the hexagonal or rectangular fin depending on the tube array arrangement. The empirical relation for the equivalent radius of a hexagonal fin, **Fig.(7.a)**, is given by:

$$\frac{r_e}{r} = 1.27 \times \psi \times (\beta - 0.3)^{1/2} \dots\dots\dots (8.c)$$

The coefficients ( $\psi$ ) and ( $\beta$ ) are defined as:

$$\psi = \frac{M}{r} = \frac{X_T}{2 \times r} \dots\dots\dots (8.d)$$

$$\beta = \frac{L}{M} = \frac{1}{X_T} \times \left[ X_L^2 + \frac{X_T^2}{4} \right] \dots\dots\dots (8.e)$$

The equivalent radius of a rectangular fin, **Fig.(7.b)**, is presented as:

$$\frac{r_e}{r} = 1.28 \times \psi \times (\beta - 0.2)^{1/2} \dots\dots\dots (8.f)$$

The coefficients ( $\psi$ ) and ( $\beta$ ) are defined as:

$$\psi = \frac{M}{r} = \frac{X_T}{2 \times r} \dots\dots\dots (8.g)$$

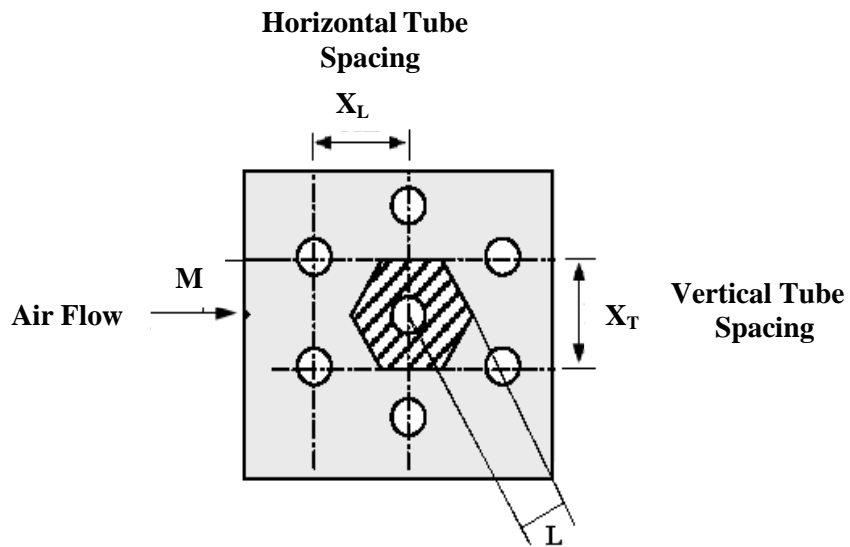
$$\beta = \frac{L}{M} = \frac{X_L}{X_T} \dots\dots\dots (8.h)$$

Once the equivalent radius has been determined, the equations for standard circular fins can be used. For the fins in this study, the length of the fin is much greater than the thickness, so a parameter ( $m$ ) can be expressed as:

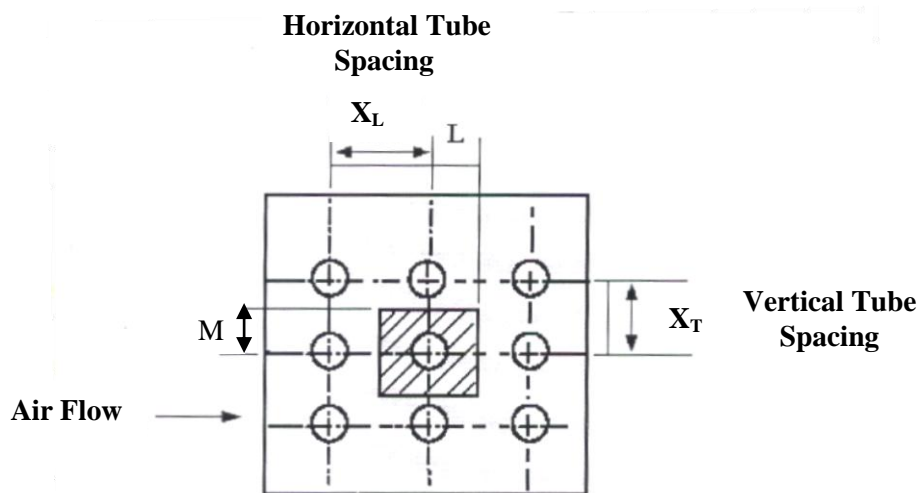
$$m = \left( \frac{2 \times h_o}{k_s \times t} \right)^{1/2} \dots\dots\dots (8.i)$$

For circular tubes, a parameter ( $\phi'$ ) is defined as:

$$\phi' = \left[ \frac{r_e}{r} - 1 \right] \left[ 1 + 0.35 \times \ln \left( \frac{r_e}{r} \right) \right] \dots\dots\dots (8.j)$$



**a) Hexangular tube array**



**b) Rectangular tube array**

**Figure (7) Continuous plate fin tube, Schmidt [11]**

## 4. Air Side Heat Transfer Correlation

### 4-1 Available Correlations

Most of the available empirical correlations for the prediction of the air side heat transfer coefficient in finned tube bank are based on fitting the data to a postulated expression depends on dimensionless groups. Heat transfer from banks of tubes is a function of multiple factors, including fin geometry, bank geometry, number of rows, physical properties, and the velocity of the heat carrier.

For radial high finned tubes in cross flow of an in-line tube arrangement a correlation was performed by Schmidt <sup>[12]</sup> in the form:

$$\mathbf{Nu} = \mathbf{0.3Re}^{0.625} \boldsymbol{\alpha}^{-0.375} \mathbf{Pr}^{0.333} \dots\dots\dots (9)$$

where,  $\alpha = A_o/A_t$

Equation (9) is valid for the following condition:  $5 < \alpha < 12$  and  $5 \times 10^3 < Re < 10^5$

For the staggered tube arrangement the average Nusselt number for finned tubes in a bank in cross flow of a gas can be calculated by:

$$\mathbf{Nu} = \mathbf{0.19} \left(\frac{\mathbf{a}}{\mathbf{b}}\right)^{0.2} \left(\frac{\mathbf{fp}}{\mathbf{D}_o}\right)^{0.18} \left(\frac{\mathbf{l}}{\mathbf{D}_o}\right)^{-0.14} \mathbf{Re}^{0.65} \mathbf{Pr}^{0.33} \dots\dots\dots (10)$$

where,  $a = X_T / D_o$  and  $b = X_L / (2D_o)$

Equation (10) is valid in the Reynolds number range  $10^2 < Re < 2 \times 10^4$

The Reynolds number of the air flowing across the tube bank in equations (9 & 10) is based on the maximum air velocity which occurs at the minimum free cross section of the finned tube bank.

At high Reynolds numbers the flow is connected with high pressure gaseous flows, which are used to increase thermal efficiency of banks. Results of Stasiulevicius <sup>[13]</sup> for inner rows of staggered banks of finned tubes with helical drafted fins (the angle of attack is less than 4°) yielded the following general equations:

$$\mathbf{Nu} = \mathbf{0.05} \left(\frac{\mathbf{a}}{\mathbf{b}}\right)^{0.2} \left(\frac{\mathbf{fp}}{\mathbf{D}_o}\right)^{0.18} \left(\frac{\mathbf{l}}{\mathbf{D}_o}\right)^{-0.14} \mathbf{Re}^{0.8} \mathbf{Pr}^{0.36} \dots\dots\dots (11)$$

In the Reynolds number range  $2 \times 10^4 < Re < 2 \times 10^5$

$$\mathbf{Nu} = \mathbf{0.008} \left(\frac{\mathbf{a}}{\mathbf{b}}\right)^{0.2} \left(\frac{\mathbf{fp}}{\mathbf{D}_o}\right)^{0.18} \left(\frac{\mathbf{l}}{\mathbf{D}_o}\right)^{-0.14} \mathbf{Re}^{0.95} \mathbf{Pr}^{0.36} \dots\dots\dots (12)$$

In the Reynolds number range  $2 \times 10^5 < Re < 2 \times 10^6$

These equations are applicable for

$2.17 < a < 4.13$ , and  $1.27 < b < 2.14$ ,  $0.125 < (X_T / D_o) < 0.28$ , and  $0.125 < (l / D_o) < 0.59$

## 4-2 Present Correlation

### 4-2-1 Formulation of the Correlation

In the present work, it is suggested to develop an empirical correlation for the air side heat transfer coefficient. This formula is based on the employment of a dimensional analysis with Buckingham-pi theorem. As it is shown above, it is quite clear that the Nusselt number for finned tube bank heat exchanger can be expressed in the following form:

$$Nu = C_f Re^i Pr^j \dots\dots\dots (13)$$

Here, the indices, (i) and (j), and the coefficient, ( $C_f$ ), are constants to be determined from experimental data for a specified finned tube and bank geometry. The coefficient, ( $C_f$ ), is a function of the finned tube geometry and bank arrangement in the form:

$$C_f = C_f(X_T, X_L, fp, l, D_o) \dots\dots\dots (14)$$

Therefore, combining eq.(13) and eq.(14) yields the following expression for the Nusselt number of air stream passing through the tube bank:

$$Nu = Nu(X_T, X_L, fp, l, D_o, Re, Pr) \dots\dots\dots (15)$$

The dimensional analysis formulated for this object generated the following dimensionless groups arranged as:

$$\pi_1 = Nu \dots\dots\dots (16.a)$$

$$\pi_2 = (X_T / X_L) \dots\dots\dots (16.b)$$

$$\pi_3 = (fp / D_o) \dots\dots\dots (16.c)$$

$$\pi_4 = (l / D_o) \dots\dots\dots (16.d)$$

$$\pi_5 = Re \dots\dots\dots (16.e)$$

$$\pi_6 = Pr \dots\dots\dots (16.f)$$

This presentation for the suggested correlation can be expressed as:

$$\mathbf{Nu} = \phi[(\mathbf{X}_T / \mathbf{X}_L), (\mathbf{fp} / \mathbf{D}_o), (\mathbf{l} / \mathbf{D}_o), \mathbf{Re}, \mathbf{Pr}] \dots\dots\dots (17.a)$$

This expression can be presented in the following form by using the constant of proportionality as:

$$\mathbf{Nu} = \mathbf{C} \left( \frac{\mathbf{X}_T}{\mathbf{X}_L} \right)^m \left( \frac{\mathbf{fp}}{\mathbf{D}_o} \right)^n \left( \frac{\mathbf{l}}{\mathbf{D}_o} \right)^k \mathbf{Re}^i \mathbf{Pr}^j \dots\dots\dots (17.b)$$

The constant of proportionality, (C), and the indices of the dimensionless groups, (i), (j), (m), (n), and (k), should be obtained from experimental data available of the present work for the cross flow finned tube banks.

The above formula is intended to be for a circular tube arrays. However, it may be used for other tube shapes if the cross sectional area was replaced by a circular one having the same mass flow rate and velocity. Hence an equivalent diameter can be induced to be used for the Nusselt number prediction of eq.(17.b).

**4-2-2 Determination of the Constants**

The indices of the Reynolds and Prandtl numbers have been inferred from the available correlations for the circular and the work of McQuiston for the plate fins outlined above. The power of the Reynolds number, (i), in eq.(17.b) has the range from (0.6 to 0.9) for most of the available correlations. Rearranging eq.(7) which is postulated by <sup>[10]</sup> to give the following form:

$$\mathbf{Nu} = \mathbf{a}_1 \mathbf{Re}^{0.6} \mathbf{Pr}^{1/3} \dots\dots\dots (18)$$

In which (a<sub>1</sub>) is a constant depends on the finned tube and bank geometry. It is obvious that the Nusselt number is proportional to Reynolds number with its power of (0.6) for the plate fin. Therefore, the value of (0.6) for the index (i) will be selected for the present work. The Prandtl number index (j) is ranged from (0.33 to 0.36) as indicated by equations (9, 10, 11, 12 and 18) for the previous correlations. A value of (0.33) may be chosen for the Prandtl number index.

The rest of the constants, (C), (m), (n), (k), presented in eq.(17) are determined from experimental data. Therefore, the suggested correlation for the prediction of the heat transfer coefficient of air passing through a plate finned tube bank of the large heat exchanger having elliptical cross sectional shape can be expressed as:

$$\mathbf{Nu} = 0.065 \times \left( \frac{\mathbf{X}_T}{\mathbf{X}_L} \right)^{0.14} \left( \frac{\mathbf{fp}}{\mathbf{D}_o} \right)^{0.1} \left( \frac{\mathbf{l}}{\mathbf{D}_o} \right)^{-0.303} \mathbf{Re}^{0.6} \mathbf{Pr}^{0.33} \dots\dots\dots (19.a)$$

For the following application conditions:

$$X_T/X_L = 0.75, \text{ and } 3.7 \times 10^4 \leq Re \leq 5.4 \times 10^4$$

and,

$$Nu = 0.034 \times \left(\frac{X_T}{X_L}\right)^{0.11} \left(\frac{fp}{D_o}\right)^{0.13} \left(\frac{1}{D_o}\right)^{-0.16} Re^{0.6} Pr^{0.33} \dots\dots\dots (19.b)$$

For the small multi tube passes heat exchanger having circular tube section at the following conditions:

$$X_T/X_L = 0.8, \text{ and } 15.8 \times 10^4 \leq Re \leq 22.6 \times 10^4$$

The Reynolds number in this correlation is based on the maximum mass velocity where a minimum flow area is considered as shown in eq.(6). The heat transfer coefficient is estimated from the Nusselt number of the above correlations in the from:

$$h_o = \frac{k \times Nu}{D_o} \dots\dots\dots (19.c)$$

The above forms of the correlation predicted the experimental data of the overall heat transfer coefficient of the tube banks considered in the present work within (2%) of deviation calculated by:

$$\Delta U_o \% = \frac{U_{\text{predicted}} - U_{\text{experimental}}}{U_{\text{predicted}}} \times 100 \dots\dots\dots (20)$$

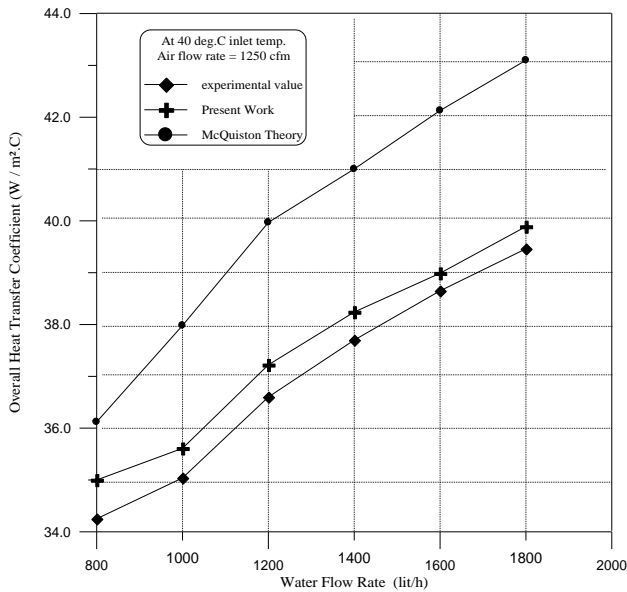
**4-3 Comparison between Experimental Data and Theoretical Prediction**

The verification of the present correlation is accomplished by introducing the predicted air side heat transfer coefficient from eq.(19) into eq.(3) for the prediction of the overall heat transfer coefficient of the heat exchanger. A comparison was made with the experimental data deduced for the present work. In addition the test data were compared with those predicted from McQuiston<sup>[10]</sup> formulation presented in eq.(7) in order to obtain a consistent verification of the present correlation with that of McQuiston formula.

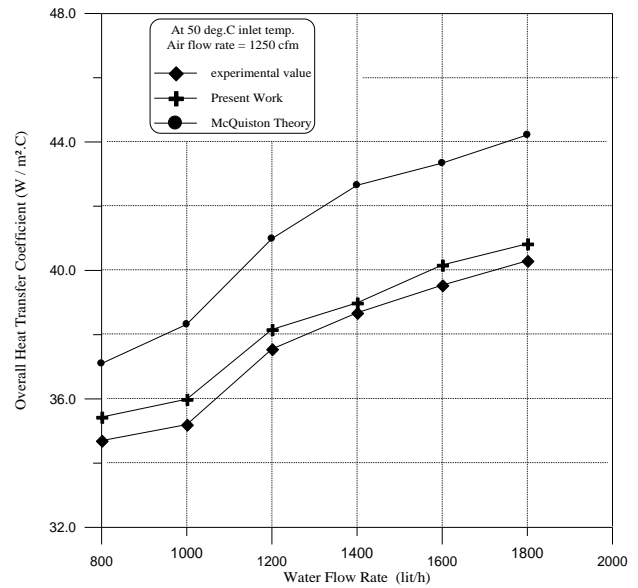
**Figure (8)** shows a comparison between the present correlation, eq.(19.a) and eq.(19.c), McQuiston correlation, eq.(7) and the experimental data of the overall heat transfer coefficient for the single pass large tube bank. The comparison of the small tube bank radiator is shown in **Fig.(9)**. It is clear that the variation of the predicted overall heat transfer coefficient has the same trend as that of the experimental data for the whole range of the tested water flow rates and temperature. The predicted values of (U<sub>o</sub>) when applying the present correlation for the air side heat transfer coefficient are closer to the experimental data than those of the McQuiston correlation for both tube banks. A comparison between the

predicted  $(U_o)_{\text{predicted}}$  and experimental data  $(U_o)_{\text{experimental}}$  of this investigation for both tube banks is shown in **Fig.(10)**. These results showed a maximum deviation of (2%) for both tube banks as calculated from eq.(20) for the whole range of operation conditions of tests.

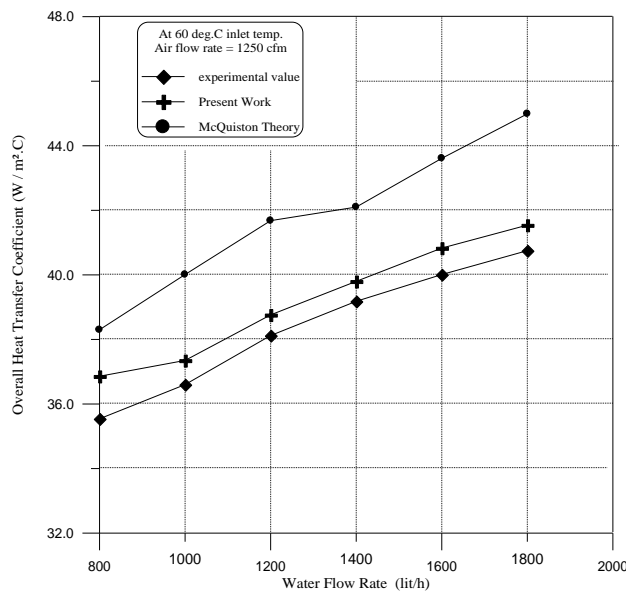
The results of the present correlation for the air side heat transfer coefficient and its role on the predicted heat exchanger duty is evident. The discrepancy between the predicted heat duty of the tube banks  $(Q)_{\text{predicted}}$  and the experimental data  $(Q)_{\text{experimental}}$  for the whole range of the water flow rates, temperature and air volumetric flow rates lies in the range of less than (4%) as shown in **Fig.(11)**.



**1) Entering water at 40 C°**

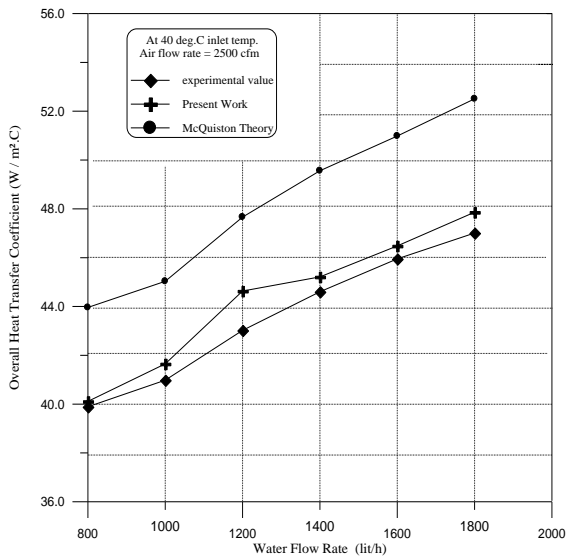


**2) Entering water at 50 C°**

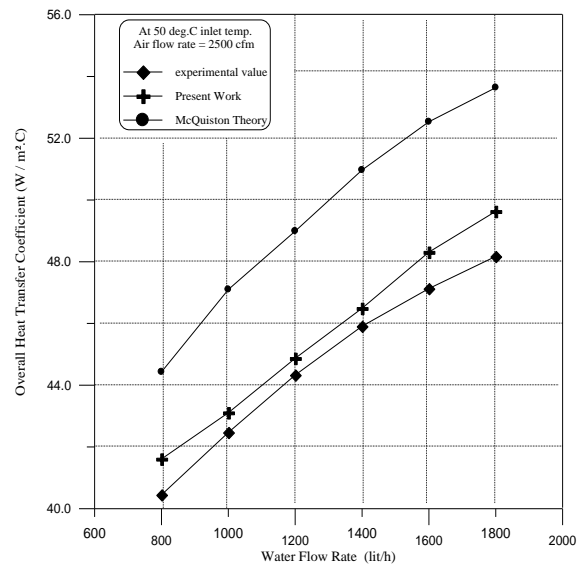


**3) Entering water at 60 C°**

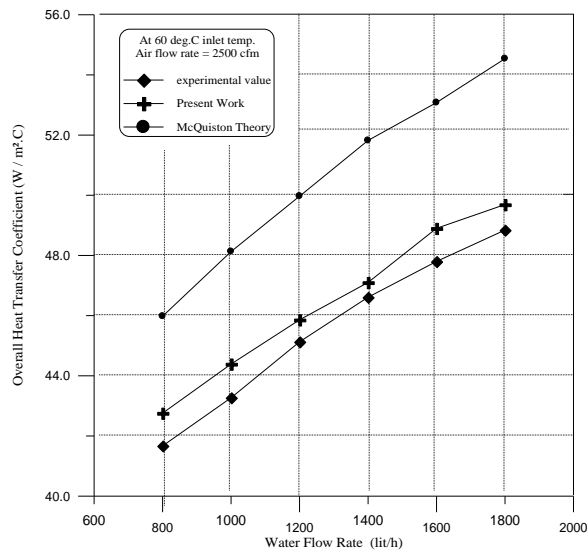
**Figure (8.a) Comparison between the experimental, present theory and McQuiston method of the overall heat transfer coefficient with water flow rate for large tube bank at 1250 cfm air flow**



**1) Entering water at 40 C°**

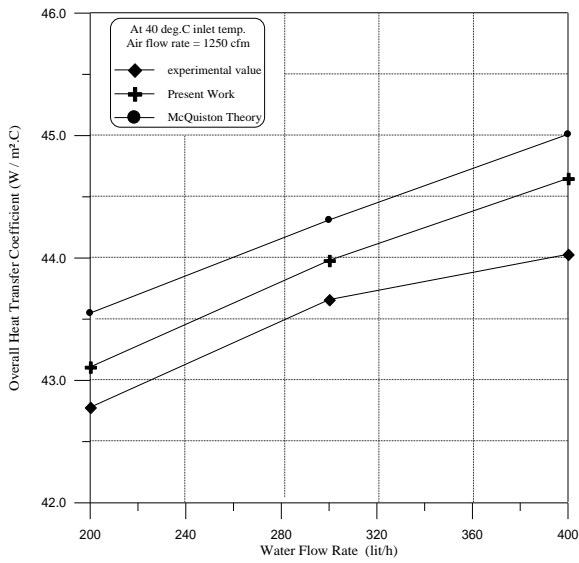


**2) Entering water at 50 C°**

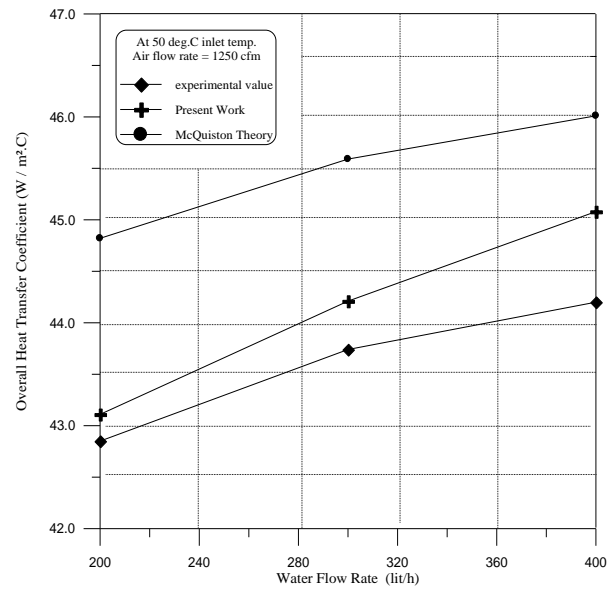


**3) Entering water at 60 C°**

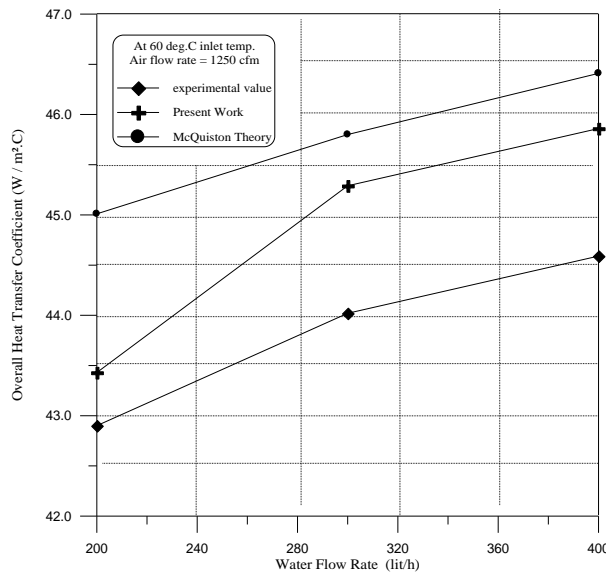
**Figure (8.b) Comparison between the experimental, present theory and McQuiston method of the overall heat transfer coefficient with water flow rate for large tube bank at 2500 cfm air flow**



**1) Entering water at 40 C°**

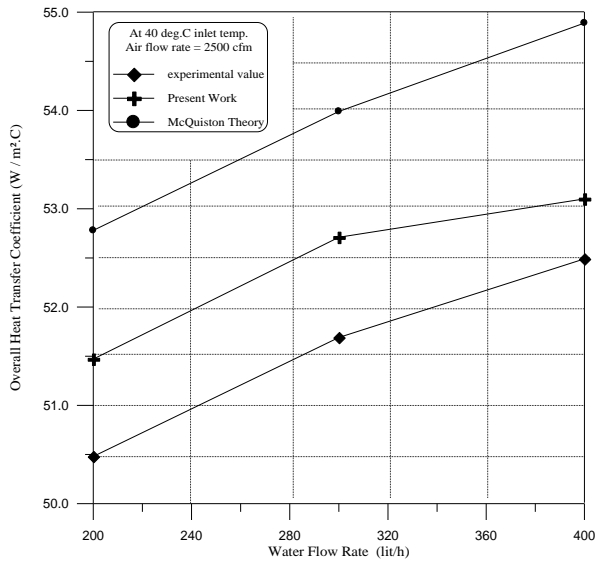


**2) Entering water at 50 C°**

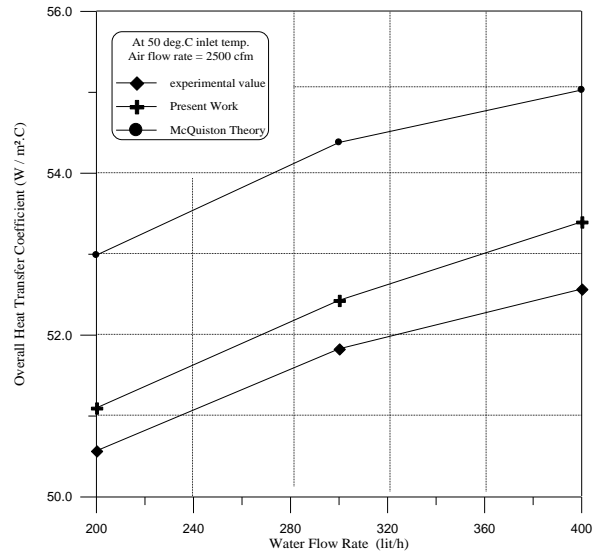


**3) Entering water at 60 C°**

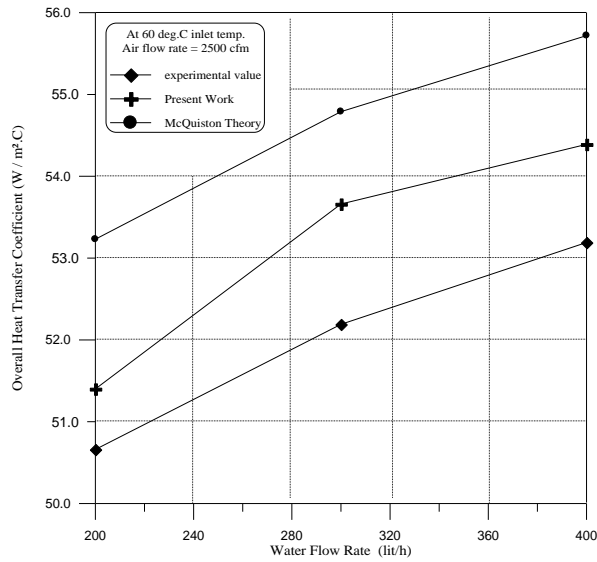
**Figure (9.a) Comparison between the experimental, present theory and McQuiston method of the overall heat transfer coefficient with water flow rate for small tube bank at 1250 cfm air flow**



**1) Entering water at 40 C°**

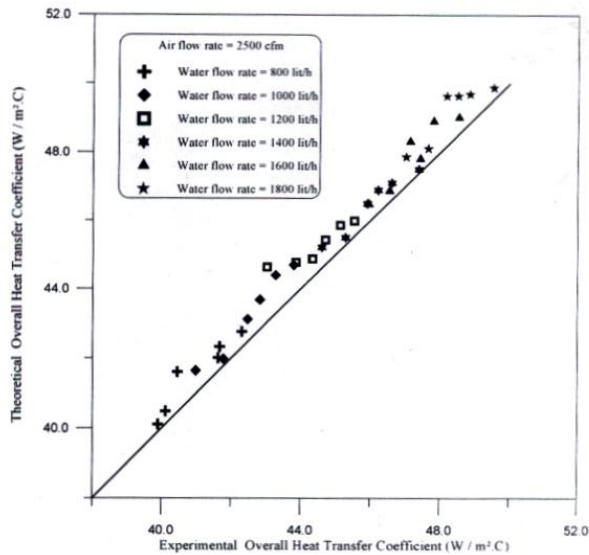


**2) Entering water at 50 C°**

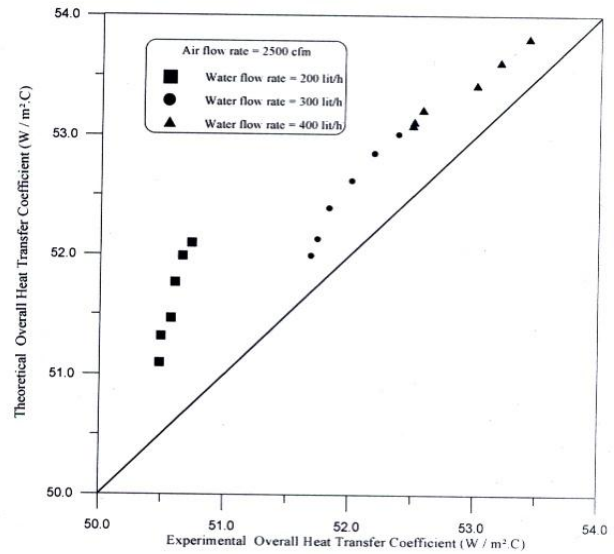


**3) Entering water at 60 C°**

**Figure (9.b) Comparison between the experimental, present theory and McQuiston method of the overall heat transfer coefficient with water flow rate for small tube bank at 2500 cfm air flow**

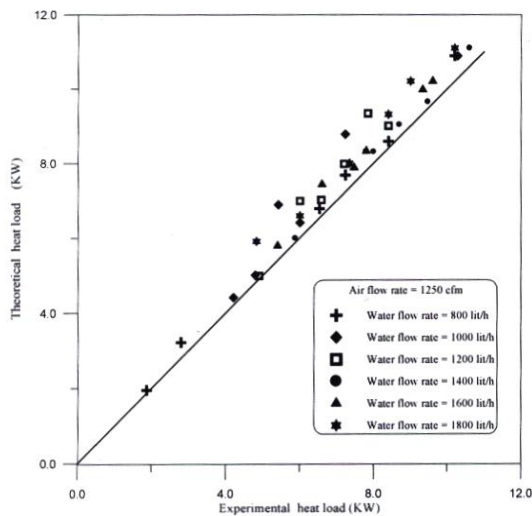


a) Large tube bank-single tube pass

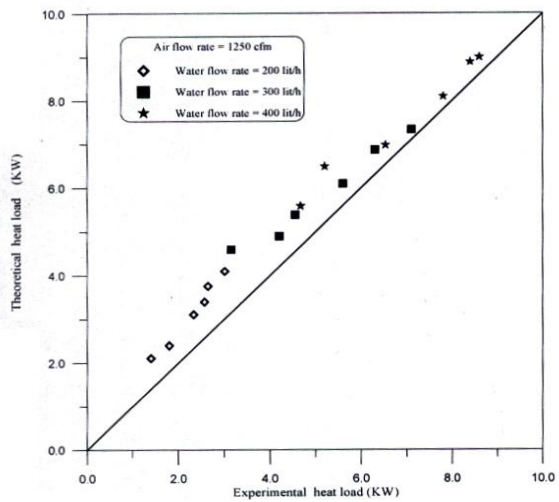


b) Small tube bank-multi tube passes

Figure (10) A comparison between the experimental data the prediction of the present work heat exchanger overall heat transfer coefficient



a) Large tube bank-single tube pass



b) Small tube bank-multi tube passes

Figure (11) A comparison between the experimental data and the prediction of the present work heat exchanger heat load

## **5. Conclusions**

The air cooled cross flow heat exchangers tested in the present work revealed that:

1. The overall heat transfer coefficient of the plate finned tube bank is controlled by the air side heat transfer coefficient. The latter was ranged between (34) and (50)  $W/m^2 K$  for the whole range of variables used in the tests for the large tube bank. The corresponding values of the small heat exchanger were (42) and (53)  $W/m^2 K$ .
2. The present suggested simplified correlation for the air side heat transfer coefficient predicted the experimental data of the overall heat transfer coefficient within acceptable accuracy. Further it is agreed well with that of McQuiston <sup>[10]</sup> method from the trend point of view but with different values. The present correlation prediction was closer than that of McQuiston correlation to the whole range of the experimental data.
3. The concept of the dimensional analysis applied in this investigation based on the Buckingham-pi theorem introduced a new perspective design correlation for the air side in the air cooled heat exchanger performance prediction.
4. For further work, it is suggested to examine the present correlation of the air side heat transfer coefficient, eq.(19), with other air side Reynolds number and tube layout geometry ratio ( $X_T/X_L$ ). This is to extend the range of application of the above correlation.

## **6. References**

1. Kakac, S., Bergles, A. E., and Mayinger, F., "*Heat Exchanger Thermal Hydraulic Fundamentals and Design*", McGraw-Hill Book Company, 1981.
2. Sinnott, R. K., "*Chemical Engineering*", Vol. 6, Heaton, A. W., and Co. LTD, Exeter, 1983.
3. Brown, R., "*A Procedure for Preliminary Estimates of Air Cooled Heat Exchangers*", in Chemical Engineering, McGraw-Hill Publication Book Co., Newyork, 1979, pp. 412-417.
4. Ganapathy, V., "*Process-Design Criteria of Air Cooled Heat Exchangers*", in Chemical Engineering, McGraw-Hill Publication Book Co., Newyork, 1979, pp. 418-425.
5. Saddler, E. M., "*Design Analysis of a Finned Tube Condenser for a Residential Air Condition Using R-22*", M.Sc. Thesis, Mech. Eng. Dept., Georgia Institute of Technology, April, 2000.
6. Stewart, S. W., Shelton, S. V., and Aspelund, K. A., "*Finned Tube Heat Exchanger Optimization*", 2<sup>nd</sup> International Conference on Heat Transfer, Fluid Mechanics and Thermodynamics, Paper Number SS2, Victoria Falls, Zambia, 23-26 June, 2003.

7. Tarrad, A. H., and Shehhab, U. S., "The Prediction of Environment Effect on the Performance of a Vapor Compression Refrigeration System in Air Conditioning Application", Engineering and Development Journal, Vol. 11, No. 1, March 2007.
8. Sieder, E. N., and Tate, C. E., "*Heat Transfer and Pressure Drop of Liquids in Tubes*", Ind. Eng. Chem., Vol. (28), 1936, pp. 1429.
9. Dittus, F. W., and Boelter, L. M. K., University of California (Berkeley), Pub. Eng., Vol. 2, 1930, pp. 443.
10. McQuiston, F. C., "*Heating Ventilating and Air Conditioning*", Analysis and Design, 3<sup>rd</sup> Edition, 1988.
11. Schmidt, T. E., "*La Production Calorifique des Surface Munies D'ailettes*", Annexe Du Bulletin De L'Institut International Du Froid, Annexe G-5, 1946.
12. Schmidt, T. E., "*Der Wärmeübergang an Rippenrohren und die Berchnung von Rohründel-Wämeaustauschern, Kältetech*", Vol. 15, No. 4, 1963, pp. 98-102, and No. 12, pp. 370-378.
13. Stasiulevicius, J., and Skrinska, A., "*Heat Transfer in Banks of Finned Tubes in Cross Flow*", Mintis, Vilnius, 1974, pp. 191-194.

## ***Nomenclature***

- A: Area, (m<sup>2</sup>)  
c: Heat capacity, (kW/C<sup>0</sup>)  
C: Constant in eq.(17.b)  
C<sub>f</sub>: Coefficient defined by eq.(14)  
c<sub>p</sub>: Specific heat, (kJ/kg. C<sup>0</sup>)  
D: Tube diameter, (m)  
fp: Fin pitch, (m)  
G: Mass velocity, (kg/m<sup>2</sup> s)  
h: Heat transfer coefficient, (W/m<sup>2</sup> K)  
H: Heat exchanger height, (m)  
h<sub>f</sub>: Fouling resistance, (W/m<sup>2</sup> K)  
i: Constant in eq.(17.b)  
j: Colburn j-factor defined by eq.(7.b), or constant in eq.(17.b)  
k: Thermal conductivity, (W/m K), or constant in eq.(17.b)  
l: Height of circular fin or plate fin length in the flow direction, (m)  
L: Tube length, (m)  
m: Constant in eq.(17.b) , or parameter defined by eq.(8.i)  
*m* : Mass flow rate, (kg/s)

n: Number of tube rows or constant in eq. (17.b)  
N<sub>circ</sub>: Number of tube circuits in heat exchanger  
NTU: Number of transfer units defined by eq. (1.g)  
P: Pressure, (bar)  
Q: Heat transfer rate, (kW)  
r: Radius of circular fin, (m)  
t: Fin thickness, (m)  
T: Temperature, (C°)  
ΔT: Temperature difference, (deg C)  
u: Fluid velocity, (m/s)  
U: Overall heat transfer coefficient, (W/m<sup>2</sup> K)  
W: Heat exchanger width, (m)  
X<sub>L</sub>: Longitudinal tube spacing in the flow direction, (m)  
X<sub>T</sub>: Transverse tube spacing perpendicular to the flow direction, (m)

### ***Subscript***

a: Air  
ad: Air dry bulb  
aw: Air wet bulb  
c: Cold side  
D: Value calculated at outside diameter  
e: Equivalent value  
f: Fin value or defined elsewhere  
h: Hot side  
i: Inlet or inside value  
min: Minimum  
max: Maximum  
o: Outside, outlet or defined elsewhere  
r: Ratio value  
s: Surface value or measured at surface condition  
t: Total or bare tube value  
w: Water side

### ***Greek Symbols***

$\alpha$ : Parameter defined in eq.(9)

$\beta$ : Parameter defined by eq.(8.e) and eq. (8.h)

$\eta$ : Efficiency

$\psi$ : Parameter defined by eq.(8.d) and eq.(8.g)

$\phi'$ : Parameter defined by eq.(8.j)

$\varepsilon$ : Heat exchanger effectiveness

$\mu$ : Fluid viscosity, (Pa.s)

$\rho$ : Fluid density, (kg/m<sup>3</sup>)

$\tau_p$ : Number of tubes per circuit